

# 3D Pre- vs. Post-Season Comparisons of Surface and Relative Pose of the Corpus Callosum in Contact Sport Athletes

Yi Lao<sup>1,2</sup>, Niharika Gajawelli<sup>1,2</sup>, Lauren Haas<sup>2</sup>, Bryce Wilkins<sup>1,2</sup>, Darryl Hwang<sup>2</sup>, Sinchai Tsao<sup>2</sup>, Yalin Wang<sup>4</sup>, Meng Law<sup>\*2,3</sup>, and Natasha Leporé<sup>\*1,2,3</sup>

<sup>1</sup>Department of Radiology, Children's Hospital Los Angeles, Los Angeles CA, USA

<sup>2</sup>Department of Biomedical Engineering, University of Southern California, Los Angeles CA, USA

<sup>3</sup>Department of Radiology, Keck School of Medicine, University of Southern California, Los Angeles, CA, USA

<sup>4</sup>School of Computing, Informatics, and Decision Systems Engineering, Arizona State University, Tempe, AZ, USA

## 1 Abstract

Mild traumatic brain injury (MTBI) or concussive injury affects 1.7 million Americans annually, of which 300,000 are due to recreational activities and contact sports, such as football, rugby, and boxing[1]. Finding the neuroanatomical correlates of brain TBI non-invasively and precisely is crucial for diagnosis and prognosis. Several studies have shown the influence of traumatic brain injury (TBI) on the integrity of brain WM [2–4]. The vast majority of these works focus on athletes with diagnosed concussions. However, in contact sports, athletes are subjected to repeated hits to the head throughout the season, and we hypothesize that these have an influence on white matter integrity. In particular, the corpus callosum (CC), as a small structure connecting the brain hemispheres, may be particularly affected by torques generated by collisions, even in the absence of full blown concussions.

Here, we use a combined surface-based morphometry and relative pose analyses, applying on the point distribution model (PDM) of the CC, to investigate TBI related brain structural changes between 9 pre-season and 9 post-season contact sport athlete MRIs. All the data are fed into surface based morphometry analysis and relative pose analysis. The former looks at surface area and thickness changes between the two groups, while the latter consists of detecting the relative translation, rotation and scale between them.

## 2 Description of purpose

TBI may lead to brain white matter injuries and disruptions, and thus temporarily or permanently impair brain function [2, 3, 5]. In-vivo imaging with MRI may be used to detect changes of brain structures in shape and relative position to better understand the impact of TBI on brain anatomy. However, to our knowledge, the relative pose of brain structures has not yet been studied in TBI. Additionally, we use a new surface based method, multivariate tensor-based morphometry (mTBM)[6] to study the full 3D structure of the CC.

Being the largest WM structure in the brain, the CC bridges the left and right hemisphere of the brain through transverse WM fibers. The midline location and intricate pathways make CC particularly vulnerable to the shear of nerve fibers resulting from traumatic axonal injury [7]. Thus, the CC is likely a sensitive indicator of brain TBI, in terms of changes in size, shape and relative pose. Using brain structural MRI, we perform regional group comparisons of the surface-morphometry and relative pose of CC between pre-season and post-season contact sport athletes. Statistic analyses are conducted using a multivariate surface-based morphometry analysis, indicating regional differences on the shape of CC, and a similarity transformation based pose analysis, indicating the changes on the relative pose of CC. We hypothesize that there may be subtle differences between pre- and posts-season contact sport participants in both shape and relative pose caused by repeated physical impact.

## 3 Method

18 T1-weighted MRI scans of collegiate contact sport athletes (9 pre-season scans and 9 post-season scans) were acquired on a 3T GE HDxT scanner. After pre-processing, including skull stripping and bias correction, the data

\*equal last author contribution

were registered to the same template space through linear registration. The CCs were then manually traced on the linear registered T1 images, and the intra-rater percentage overlap was 0.937, with four participants at two different intervals. Subsequently, 3D surface representations and mesh grids of the CC were constructed using our in-house conformal mapping program. One-to-one correspondence between vertices were obtained through a surface fluid registration algorithm [8].

### 3.1 Surface based morphometry analysis

Surface based morphometry analysis is achieved by a vertex-wise multivariate statistical analysis of radial distance and logged deformation tensor [6]. Initially, a surface grid is generate on the CCs, and linear registration and surface based fluid registration are computed to remove the irrelevant global pose information and obtain correspondence in vertices.

The radial distance is computed as the distance of the medial axis to each vertex, which primarily measures changes along the surface normal direction of a given vertex. Complementary to this commonly used morphometry measurement, we also include the deformation tensors ( $\sqrt{JJ^T}$ ), where  $J$  is the Jacobian of the deformation transforming all CCs to a common space), which is induced in the surface fluid registration. Since the deformation tensors are positive definite matrices, which do not form a vector space, all the deformation tensors are projected onto a log-Euclidean space-the tangent plane at the origin of the manifold of deformation tensors-for future statistical analysis. To perform a combined radial distance and multivariate tensor-based morphometry, we define a 4 x 1 feature vector consisting of the radial distance (1 x 1) and the logged deformation tensor (3 x 1) on each of the surface vertices. Group statistics are computed using the Hotelling's T2 test, which is a multivariate generalization of the  $t$ -test, and followed by two permutation tests: a vertex-based one to avoid the normal distribution assumption, and one over the whole segmented image to correct for multiple comparisons[9].

### 3.2 Relative pose analysis

For each CC, the relative pose was obtained by a full Procrustes fit of a template shape to the PDM[10, 11]. The template shape was selected as the mean shape that minimized the Procrustes distances, and it was computed iteratively. The transformation rule of Procrustes alignment is defined as,  $T(X)=(sRX, d)$ , where  $s$  is the scalar scaling factor,  $R$  is a  $3 \times 3$  rotation matrix and  $d$  is the translation vector  $(x, y, z)^T$  [12]. To form a Lie group with matrix multiplication [13], the matrix representation of the Procrustes transformation can be written as:

$$T = \begin{pmatrix} sRX & d \\ 0^T & 1 \end{pmatrix} \quad (1)$$

To simplify computations, all the parameters of the transformations were projected onto a log-Euclidean space. The mean pose in the log-Euclidean space can be calculated iteratively as in [14]:

$$m_{k+1} = m_k \exp\left(\frac{1}{n} \sum_{i=1}^n \log(m_k^{-1}T_i)\right). \quad (2)$$

After the subtraction of the mean ( $m$ ) from each subject's individual pose, specifically using  $v_i = \log(m^{-1}T_i)$ , each subject is left with a residual pose. Statistics are computed on the residual pose which consists of 7 parameters: 1 scale scalar, 3 rotation scalars and 3 translation scalars.

Statistical comparisons between the two groups were performed via two methods: univariate  $t$ -test for  $\log S$ ,  $||\log R||$ ,  $||\log d||$ ,  $\theta_x, \theta_y, \theta_z$ ,  $x, y, z$ ; multivariate Hotelling's  $T^2$ -test for 3 rotation parameters ( $\theta_x, \theta_y, \theta_z$ ), 3 translation parameters ( $x, y, z$ ), a combination of  $\log S$ ,  $||\log R||$ , and  $||\log d||$ , as well as a combination of all 7 parameters. Considering the limited size of our dataset, for each of the parameters, a permutation test[15, 9] with 10,000 random redistributions of the 'contact' or 'non-contact' labels was performed to avoid the normal distribution assumption.

## 4 Results

### 4.1 Surface based morphometry results

Fig. 1 shows the results of surface based morphometry analysis. As we can see, widespread areas of the CC present significant difference (which we set at  $p < 0.05$ ) between pre-season and post-season groups. Large clusters of differences were found in regions close to the splenium as well as the left and right borders of the CC.

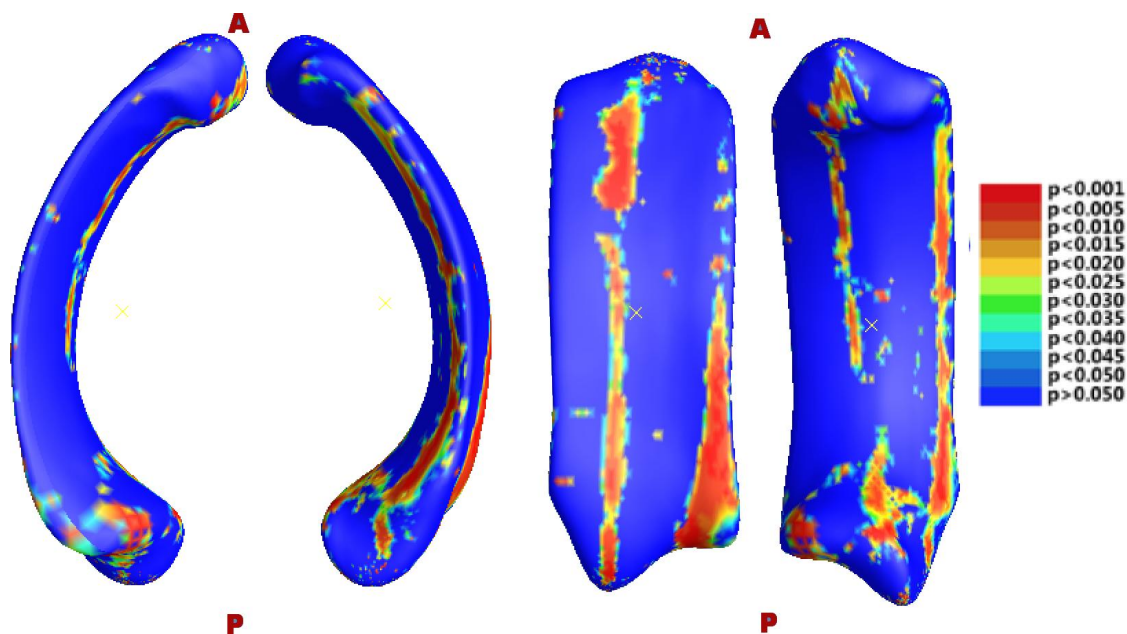


Fig. 1: Visualization of surface-based morphometry results on CC.

### 4.2 Relative pose results

All the  $p$ -values from previously described tests are presented in Table 1. As we can see from the table, pose parameters representing rotation show a significant difference between the pre-season and post-season groups, while no difference can be seen in scale and translation parameters. Additionally, a combination of all 7 parameters also detected significant differences between the two groups, indicating a possibility of using multivariate analysis of all pose parameters as the discriminant between the two populations.

These results are better visualized in Fig. 2, which shows a superimposition of the mean poses of the pre-season group (red) and post-season group (blue) respectively. The CC of the post-season group showed an left leaning tendency compared to the pre-season group, which is consistent with the differences found in rotation parameters. Compared to the obvious rotational difference, the size and translation differences in these two groups are less evident, thus further validating lack of significance results from the size and translation parameters.

Table 1: P-value of statistical analyses on pose parameters: 13 sets of parameters characterizing the relative pose of the CC are investigated here using univariate and multivariate analyses. Parameters are categorized as  $\log S$ ,  $\|\log R\|$ ,  $\|\log d\|$ ,  $\theta_x, \theta_y, \theta_z$ ,  $x$ ,  $y$ , and  $z$  for univariate tests, and as  $(\theta_x, \theta_y, \theta_z)$ ,  $(x, y, z)$ ,  $(\log S, \|\log R\|, \|\log d\|)$ , and a combination of 7 parameters for multivariate tests. All the  $p$ -values are obtained after permutation testing. Significant  $p$ -values ( $p < 0.05$ ) are highlighted in light cyan. Non significant, but interested low  $p$ -values are highlighted in light grey.

pose parameters	$p$ -values	pose parameters	$p$ -values
$\log S$	7.95e-01	$\ \log R\ $	4.39e-02
$\theta_x$	1.51e-02	$\ \log d\ $	4.70e-01
$\theta_y$	8.95e-01	$(\theta_x, \theta_y, \theta_z)$	1.10e-01
$\theta_z$	1.63e-01	$(x, y, z)$	3.11e-01
$x$	5.73e-01	$(\log S, \ \log R\ , \ \log d\ )$	2.49e-01
$y$	2.00e-01	<i>All7paras</i>	3.52e-02
$z$	1.27e-01		

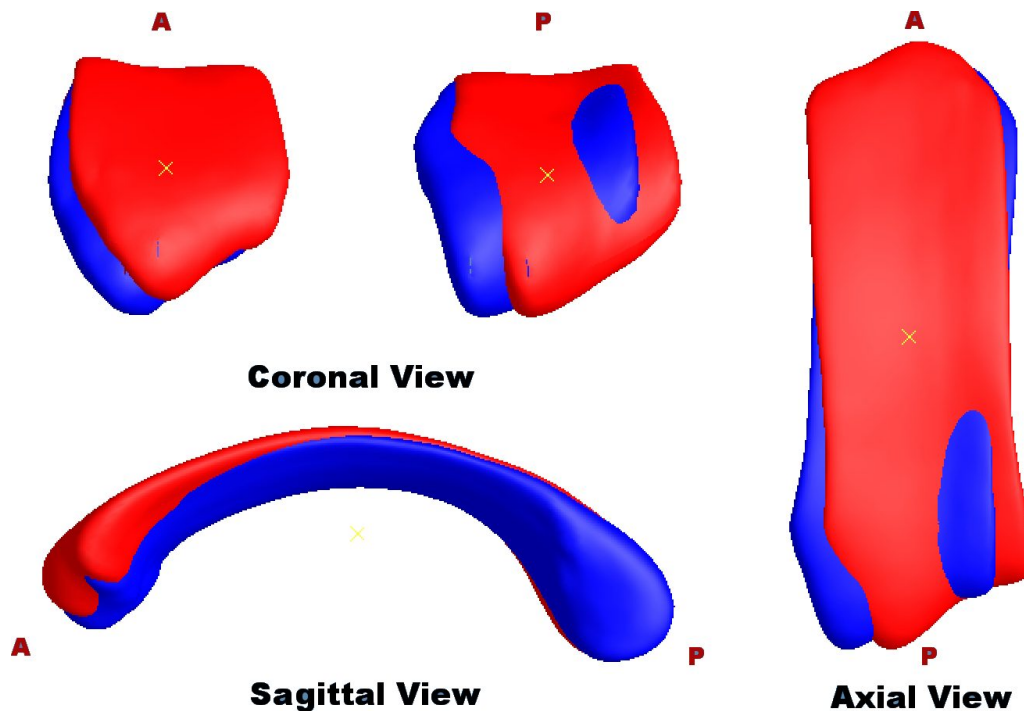


Fig. 2: 3D visualization of the mean shape of all the CCs in the mean poses averaged from pre-season group (red) and post-season group (blue) respectively. A shift in pose is evident in terms of a rotation on the anterior and posterior ends of the CC, while less visible differences can be seen in size and transformation.

## 5 New or breakthrough work to be presented

There are two major contributions in this paper. First, although surface-based shape analysis have shown high sensitivity in detecting subtle brain anatomy changes[6,16,17], it is the first time to our knowledge that it has been used in TBI studies. Second, we introduce a novel pose analysis system that integrates various brain

surface processing techniques including parametrization and surface fluid registration and reports the subtle pose changes on subcortical structures. The obtained pose information is complementary to subcortical surface shape analyses, and the combined shape and pose results form a complete subcortical morphometry system. There is little research analyzing the relative pose of brain structures in general, and none in TBI. Our work may lead to new biomarkers for TBI.

## 6 Conclusions

Here, we introduce a combined surface morphometry and relative pose analyses into the TBI associated brain anatomy analyses. Our measurements successfully detected differences in the CC between pre-season and post-season contact sport participants, in terms of changes in both shape and pose. Our study supports the concept that there are TBI related brain structural changes in contact sport athletes that may be related to repeat physical impacts. Our results provide additional information in understanding the TBI patterns, and may serve as sensitive indicators of similar kinds of brain anatomy changes. In the future, we will recruit more subjects in our study and further validate these results. In addition, we will correlate our surface based morphometry and relative pose results with the neuropsychological testing scores of these subjects.

## References

1. Bazarian, J.J., Zhu, T., Blyth, B., Borrino, A., Zhong, J.: Subject-specific changes in brain white matter on diffusion tensor imaging after sports-related concussion. *Magnetic resonance imaging* **30**(2) (2012) 171–180
2. McKee, A.C., Stein, T.D., Nowinski, C.J., Stern, R.A., Daneshvar, D.H., Alvarez, V.E., Lee, H.S., Hall, G., Wojtowicz, S.M., Baugh, C.M., et al.: The spectrum of disease in chronic traumatic encephalopathy. *Brain* **136**(1) (2013) 43–64
3. Singh, M., Jeong, J., Hwang, D., Sungkarat, W., Gruen, P.: Novel diffusion tensor imaging methodology to detect and quantify injured regions and affected brain pathways in traumatic brain injury. *Magnetic resonance imaging* **28**(1) (2010) 22–40
4. Duda, J., Avants, B., Kim, J., Zhang, H., Patel, S., Whyte, J., Gee, J.: Multivariate analysis of thalamo-cortical connectivity loss in tbi. In: *Computer Vision and Pattern Recognition Workshops, 2008. CVPRW'08. IEEE Computer Society Conference on, IEEE* (2008) 1–8
5. Gajawelli, N., Lao, Y., Apuzzo, M.L., Romano, R., Liu, C., Tsao, S., Hwang, D., Wilkins, B., Lepore, N., Law, M.: Neuroimaging changes in the brain in contact versus noncontact sport athletes using diffusion tensor imaging. *World neurosurgery* **80**(6) (2013) 824–828
6. Wang, Y., Song, Y., Rajagopalan, P., An, T., Liu, K., Chou, Y.Y., Gutman, B., Toga, A.W., Thompson, P.M.: Surface-based tbn boosts power to detect disease effects on the brain: An n= 804 adni study. *Neuroimage* **56**(4) (2011) 1993–2010
7. Wilde, E.A., Chu, Z., Bigler, E.D., Hunter, J.V., Fearing, M.A., Hanten, G., Newsome, M.R., Scheibel, R.S., Li, X., Levin, H.S.: Diffusion tensor imaging in the corpus callosum in children after moderate to severe traumatic brain injury. *Journal of neurotrauma* **23**(10) (2006) 1412–1426
8. Shi, J., Wang, Y., Ceschin, R., An, X., Nelson, M.D., Panigrahy, A., Leporé, N.: Surface fluid registration and multivariate tensor-based morphometry in newborns-the effects of prematurity on the putamen. *APSIPA Annual Summit and Conference* (2012)
9. Lepore, N., Brun, C., Chou, Y.Y., Chiang, M.C., Dutton, R.A., Hayashi, K.M., Luders, E., Lopez, O.L., Aizenstein, H.J., Toga, A.W., et al.: Generalized tensor-based morphometry of hiv/aids using multivariate statistics on deformation tensors. *Medical Imaging, IEEE Transactions on* **27**(1) (2008) 129–141
10. Ross, A.: Procrustes analysis. Course report, Department of Computer Science and Engineering, University of South Carolina (2004)
11. Dryden, I., Mardia, K.: *Statistical analysis of shape*. Wiley (1998)
12. Bossa, M., Zacur, E., Olmos, S.: Statistical analysis of relative pose information of subcortical nuclei: application on adni data. *Neuroimage* **55**(3) (2011) 999–1008
13. Bossa, M.N., Olmos, S.: Statistical model of similarity transformations: Building a multi-object pose model of brain structures. In: *IEEE Comput. Soc. Workshop Math. Methods Biomed. Image Anal.* (2006) 59
14. Pennec, X., Fillard, P., Ayache, N.: A riemannian framework for tensor computing. *International Journal of Computer Vision* **66**(1) (2006) 41–66
15. Nichols, T.E., Holmes, A.P.: Nonparametric permutation tests for functional neuroimaging: a primer with examples. *Human brain mapping* **15**(1) (2001) 1–25

16. Wang, Y., Zhang, J., Gutman, B., Chan, T.F., Becker, J.T., Aizenstein, H.J., Lopez, O.L., Tamburo, R.J., Toga, A.W., Thompson, P.M.: Multivariate tensor-based morphometry on surfaces: Application to mapping ventricular abnormalities in hiv/aids. *NeuroImage* **49**(3) (2010) 2141–2157
17. Shi, J., Wang, Y., Ceschin, R., An, X., Lao, Y., Vanderbilt, D., Nelson, M.D., Thompson, P.M., Panigrahy, A., Leporé, N.: A multivariate surface-based analysis of the putamen in premature newborns: Regional differences within the ventral striatum. *PloS one* **8**(7) (2013) e66736